Orthogonal Multicode Channelization Applied to Subsampling Digital UWB Receiver

Yves Vanderperren*, Geert Leus†, Wim Dehaene*
*EE Dept. (ESAT-MICAS), Katholieke Universiteit Leuven, Belgium
†Faculty of EE, Mathematics and CS, Delft University of Technology, The Netherlands
Email: {yves.vanderperren,wim.dehaene}@esat.kuleuven.be, leus@cas.et.tudelft.nl

***Abstract*— This paper assesses in AWGN and dense multipath environments several equalization alternatives for a digital pulsed UWB receiver sampling below Nyquist rate. A suboptimal but implementation efficient Minimum Mean-Square Error (MMSE) equalizer which reaches performances similar to the ideal MMSE equalizer is proposed. By making an efficient use of orthogonal codes, the UWB transceivers have flexible channelization means to accomodate time-varying data rate in the order of magnitude of 100 Mb/s with sampling rates below 1 GHz. The proposed multicode approach takes into account the peculiarities of pulsed UWB signals and avoids high peak-to-average amplitude ratios.**

I. Introduction

The design of UWB receivers presents unique challenges. The most popular receiver is based on matched filtering (correlation) with the transmitted pulse followed by a RAKE structure capturing the multipath diversity of the channel. However, the pulse distortion introduced by the transceiver antennas and the channel can vary among the multipaths. As a result, the RAKE receiver can not achieve the optimal performance. Transmitted reference (TR) systems [1] sample the received signal avoid the need for local template generation ans sample at the pulse repetition rate, but require extremely wideband delay lines in the analog domain which are particularly difficult to realize. On the other hand, digital based receivers provide more flexibility and benefit from CMOS technology scaling, but require ADCs sampling at Nyquist rate which are hardly realizable and highly power consuming. As the ADC power consumption of Flash ADCs, the standard solution for digital UWB architectures, scales linearly with the sampling rate and as a factor close to 4 with the bit width [2], the UWB system architect can choose either a high (Nyquist) sample rate or multi-bit resolution but not both. Several high speed 1-bit receiver architectures have been proposed, e.g. in [3], [4]. However, 1-bit receivers suffer from poor robustness against interferers, which needs to be improved using notch filters in the RF front-end or by shaping appropriately the transmitted pulse. The first solution comes at the cost of flexibility, whereas the second requires the transmitter to know the interference at the receiver via some kind of feedback loop. Parallel multi-bit ADC architectures based on signal channelization in time ([4], [5]) or frequency domain ([6], [7]) reach an aggregate sampling rate equivalent to Nyquist's criterion and support interference cancellation in the digital domain. However, this advantage comes at the cost of increased area and power consumption, as each ADC typically consumes about 100 mW using state-of-the-art Flash ADCs, see e.g. [8]. The sampling rate speed is relaxed in [4] by using a bank of discrete-frequency matched filters followed by parallel ADCs. Still, all these solutions require careful control of the circuit mismatches between the parallel branches.

Subsampling techniques provide an attractive alternative. For example, a direct sampling approach is used in [9]. However, it is only applicable for signals in the 3-5 GHz band and still requires a 2 GSamples/s ADC. In this paper, we compare different equalization techniques in the context of the subsampling receiver based on line spectrum methods proposed in [10]. Following this comparison, we improve substantially the receiver's performance without affecting its complexity. Additionally, we show how to reach data rates in the order of magnitude of 100 Mb/s with sampling rates below 1 GHz, by adopting a multicode approach which takes into account the peculiarities of pulsed UWB signals and avoids high peak-to-average amplitude ratios.

II. Application of Subsampling Techniques to Pulsed UWB Signals

A. Basic Signal Model and Subsampled Pulse Detection Algorithms

A received pulsed UWB signal $s_{rx}(t)$ can be modelled as the convolution between a stream of Diracs sent at frame rate $1/T_f$, the received pulse shape $p_{rx}(t)$, and the channel $h(t)$:

$$s_{rx}(t) = p_{rx}(t) \otimes h(t) \otimes \sum_{n=-\infty}^{+\infty} \sum_{k=1}^{K} a_{n,k} \delta(t - nT_f - t_{n,k}) + n(t) \tag{1}$$

where $a_{n,k} \in \{0, \pm A, \pm 3A, \dots\}$ and $t_{n,k} \in \{0, \Delta, 2\Delta, \dots\}$ are the data streams modulating K pulse amplitudes and positions per period T_f, respectively, and $n(t)$ is the received additive while gaussian noise (AWGN). This model is valid provided that the channel $h(t)$ does not modify the pulse shape, i.e. $h(t) = \sum_{i=1}^{N_p} \alpha_i \delta(t - \tau_i)$, where N_p is the total number of paths.

Following the work on sampling signals with finite rate of innovation [11], it has been suggested in [10], [12], [13] to apply parametric PSD estimation methods in the frequency domain to estimate the position of the Diracs. Line spectrum PSD estimation methods can be used, for example, to retrieve the position of the pulses after deconvolving the received signal by the pulse shape [13]. This operation is done by

dividing in the frequency domain the sampled received signal $FFT(s_{rx}[n])$ by the pulse spectrum $FFT(p_{rx}[n])$. However, the number of paths which contribute significantly to the received energy is very high for typical UWB channels, requiring parametric estimation methods with unafordable high order. Although a reduced set of principal components is estimated in [13], the order remains prohibitive (>10 for Channel Model 1 in [14]) and affects the receiver complexity and the sampling rate. Moreover, it is assumed that the received pulse shape is known at the receiver, while it can differ significantly from the transmitted pulse shape. Pulse distortion is caused in particular by the transceiver antennas if these do not have a constant gain and linear phase frequency response. Such distortion is hard to estimate independently from the channel effect. A more realistic model which takes into account the frequency selective distortion is given by

$$s_{rx}(t) = h_c(t) \otimes \sum_{n=-\infty}^{+\infty} \sum_{k=1}^{K} c_{n,k}\delta(t - nT_f - t_{n,k}) + n(t) \quad (2)$$

where $h_c(t) = \sum_{i=1}^{N_p} \alpha_i p_i(t - \tau_i)$ is the compound channel impulse response, which includes the distortion caused by the antennas and the dispersive behavior of the building materials in the propagation channel. The deconvolution by the pulse shape can therefore not be applied. A combination of rational PSD estimation methods and a polynomial model for the frequency domain representation of $h_c(t)$ is proposed in [15]. However, this approach also suffers from a high sampling rate caused by the required polynomial order. Instead, the authors of [10], [12] propose to deconvolve the received signal by the compound channel using a simple Zero-Forcing equalizer, and apply a line spectrum PSD estimation method of minimal order. This approach is extended in section II-C to improved equalization techniques.

B. Basic Principles of the Subsampling Receiver

The received signal $s_{rx}(t)$ is filtered and sampled following [11] and $2M{+}1$ frequency domain samples $\mathbf{y} = [y[-M], \ldots, y[M]]$ are available, with $M{\geq}K$. Let $\mathbf{H}_{fc}$ be defined as a diagonal matrix with the $2M{+}1$ frequency domain representation of the filtered compound channel. For the sake of simplicity, we consider here a single user system and do not take the PN spreading into account. The received signal in the frequency domain $\mathbf{y}$ can be expressed as

$$\mathbf{y} = T_f^{-1}\mathbf{H}_{fc}\mathbf{B}\mathbf{a} + \mathbf{n} = \mathbf{H}_{fc}\mathbf{s} + \mathbf{n} \quad (3)$$

where $\mathbf{n}$ corresponds to the filtered noise in the frequency domain, $\mathbf{B} = [\mathbf{b}_1 \ \ldots \ \mathbf{b}_K]$, $\mathbf{b_k} = \left[z_k^{-M}, \ldots, z_k^{M}\right]$ with $z_k = e^{-2\pi j t_k/T_f}$, $\mathbf{a} = [a_1, \ldots, a_K]$, and $\mathbf{s} = T_f^{-1}\mathbf{B}\mathbf{a}$. We omit n in $t_{n,k}$ and $a_{n,k}$ since we focus in this section on a single frame. The filtered compound channel impulse response $h_{fc}(t)$ is assumed available via appropriate training of the receiver using a known preamble sent at the beginning of the data stream. An equalization filter with frequency response $\mathbf{H}_{eq}$ is constructed based on this training information, and is applied to the received signal in the frequency domain: $\hat{\mathbf{s}} = \mathbf{H}_{eq}\mathbf{y}$. A conventional line spectrum method of order K, for example ESPRIT or RootMUSIC, is then applied to the equalized signal $\hat{\mathbf{s}}$ to estimate the positions $\left\{\hat{t_i}\right\}_{i=1}^{K}$. The estimated amplitudes $\{\hat{a_i}\}_{i=1}^{K}$ are given by the least-squares (LS) solution of system (3) after equalization:

$$\hat{\mathbf{a}} = T_f\mathbf{B}^{\dagger}\hat{\mathbf{s}} \quad (4)$$

C. Channel Equalization Alternatives

We consider here the particular case of linear equalizers working at symbol rate, such as Zero-Forcing (ZF) and Minimum Mean-Square Error (MMSE) equalizers. Indeed, fractionally spaced equalizers exacerbate the sampling rate issue and are not suitable for subsampling digital UWB receivers.

1) ZF: In this case, $\mathbf{H}_{eq} = \mathbf{H}_{fc}^{-1}$ and the deconvolution by $h_{fc}(t)$ is implemented as a division in the frequency domain. This simple solution requires only $(2M{+}1)$ inversions during training and $(2M{+}1)$ multiplications for each data symbol.

2) Optimal MMSE: The MMSE equalizer minimizes $\mathcal{J} = \mathrm{E}\left\{\|\mathbf{s} - \hat{\mathbf{s}}\|^2\right\}$. Solving for $\partial\mathcal{J}/\partial\mathbf{H}_{eq} = 0$, the general expression of the MMSE is given by

$$\mathbf{H}_{eq} = \left(\mathbf{H}_{fc}^H\mathbf{R}_n^{-1}\mathbf{H}_{fc} + \mathbf{R}_s^{-1}\right)^{-1}\mathbf{H}_{fc}^H\mathbf{R}_n^{-1} \quad (5)$$

where $\mathbf{R}_s{=}\mathrm{E}\left\{\mathbf{s}\mathbf{s}^H\right\}$ and $\mathbf{R}_n{=}\mathrm{E}\left\{\mathbf{n}\mathbf{n}^H\right\}$ are the data and noise covariance matrices in the frequency domain. This equalizer involves the inversion of a $(2M{+}1)$-by-$(2M{+}1)$ matrix, as

$$\mathbf{H}_{eq} = \mathbf{R}_s\mathbf{H}_{fc}^H\left(\mathbf{H}_{fc}\mathbf{R}_s\mathbf{H}_{fc}^H + \mathbf{R}_n\right)^{-1} \quad (6)$$

using the matrix inversion lemma. The equalization of each data symbol $\mathbf{y}$ by $\mathbf{H}_{eq}$ requires $2(2M{+}1)^2$ operations.

3) Suboptimal MMSE: Provided that the pulse shape has a flat spectrum in the band selected by the receiver bandwidth, we can relax the assumption of colored noise and signal covariance matrices. By approximating $\mathbf{R}_s$ and $\mathbf{R}_n$ with their diagonal only, (6) requires then only the inversion of $2M{+}1$ numbers, since $\mathbf{H}_{fc}$ is already diagonal. The estimation of the approximated noise covariance matrix $\mathbf{R}_{n,diag}{=}\sigma_n^2\mathbf{I}_{2M+1}$ requires only the estimation of the noise power at the equalizer input, which can be done during training. The approximated signal covariance matrix $\mathbf{R}_{s,diag} = \sigma_s^2\mathbf{I}_{2M+1}$ is known at the receiver since it corresponds to the power of the transmitted pulse. This assumption is valid provided that the Voltage Gain Amplifier (VGA) sets the signal power at a known reference level according to the Automatic Gain Control (AGC), irrespective of the received power at the antenna. Otherwise the signal power at the equalizer input must be estimated as well. Defining $SNR{=}\sigma_s^2/\sigma_n^2$, the suboptimal MMSE equalizer can be expressed as

$$\mathbf{H}_{eq} = \mathbf{H}_{fc}^H\left(\mathbf{H}_{fc}\mathbf{H}_{fc}^H + SNR^{-1}\mathbf{I}_{2M+1}\right)^{-1} \quad (7)$$

and only involves the manipulation of complex numbers with a complexity of $\mathcal{O}(2M+1)$. The equalization of each data symbol requires $(2M{+}1)$ multiplications, like the ZF equalizer.

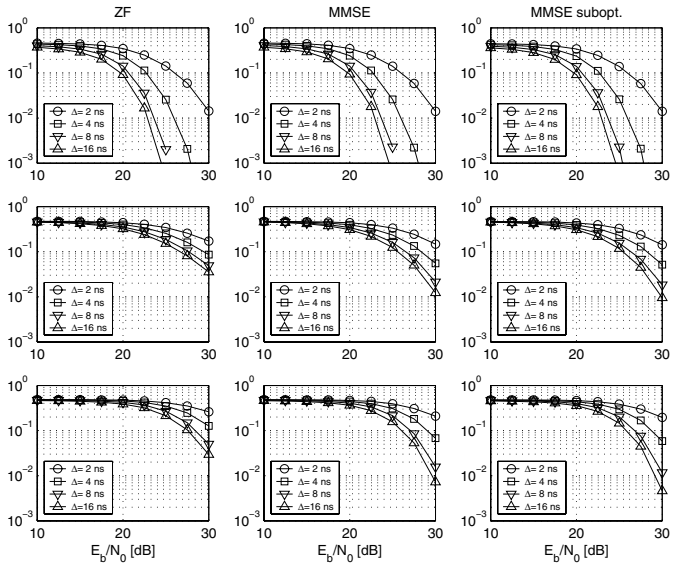

Fig. 1. BER PPM, $f_s = 312.5$ MHz, for AWGN channel (top), CM1 averaged over 100 realizations (middle), CM1 realization 1 (bottom).

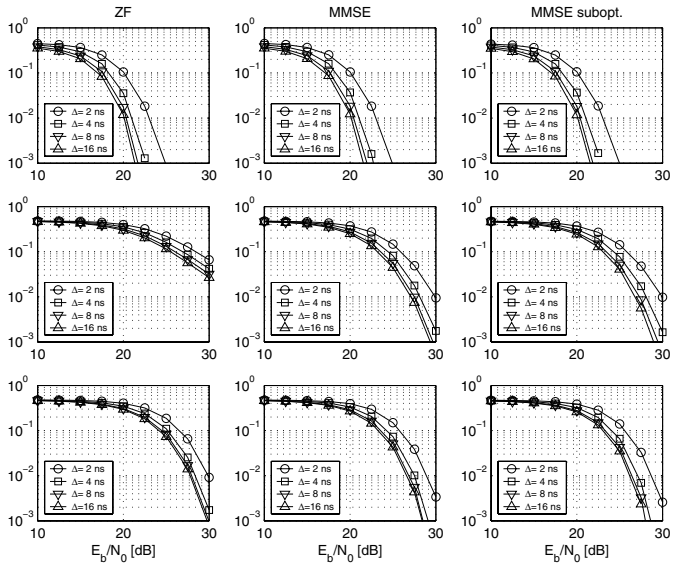

Fig. 2. BER PPM, $f_s = 625$ MHz, for AWGN channel (top), CM1 averaged over 100 realizations (middle), CM1 realization 1 (bottom).

D. Performance of the Equalization Alternatives

A subsampling receiver based on ESPRIT has been simulated with an AWGN channel and multipath conditions [14]. Given a desired $(E_b/N_0)_{des}$, the AWGN noise power σ_n^2 added to the receiver input signal is such that $(E_b/N_0)_{des} = \left(\sigma_s^2/\sigma_n^2\right) T_f W$, where σ_s^2 is the average signal power and W the model bandwidth. This definition of SNR allows for a fair comparison of the receiver performance when using different filter bandwidths and sampling rates f_s. The simulation results presented in this paper have been obtained with the second derivative of the gaussian monocycle, but no significant difference was observed with other pulses. A single pulse per period ($K = 1$) is assumed for simplicity. The pulse repetition period is high enough ($T_f = 51.2$ ns for CM1) to avoid inter pulse interference (IPI). The central frequency f_c of the receiver bandpass filter is chosen as the maximum of the pulse PSD.

Figures 1–3 illustrate the BER curves for PPM for various sampling rates as a function of the modulation index Δ. The MMSE and ZF equalizers present the same performance in AWGN channels since only the pulse PSD, which is almost flat in the considered band, is equalized. When considering realistic multipath conditions, such as CM1, which present numerous amplitude dips in their frequency response, the ZF may still be close to the MMSE for particular channel realizations. However, the MMSE outperforms the ZF equalizer when the results are averaged over several realizations. The noise power term in (6) and (7) prevents noise enhancement at these locations, as confirmed by the increasing performance improvement of the MMSE vs. the ZF equalizer for larger receiver bandwidths and sampling rates. Interestingly, the suboptimal MMSE based on diagonal covariance matrices does not introduce any BER penalty for the sampling rates which allow for reliable communication, i.e. $M_{min} \approx 8$ or $f_{s,min} \approx 16/T_f$. Indeed, the receiver bandwidth is then high enough, compared to the pulse repetition rate, to guarantee almost diagonal signal and noise covariance matrices.

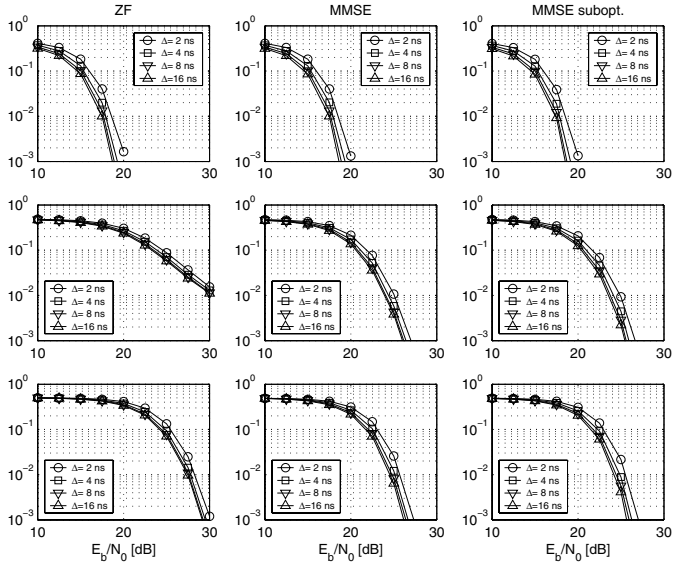

Fig. 3. BER PPM, $f_s = 1250$ MHz, for AWGN channel (top), CM1 averaged over 100 realizations (middle), CM1 realization 1 (bottom).

The comments for PAM modulation (fig. 4) are similar to PPM. The superior results of the MMSE vs. the ZF equalizer for increasing bandwidth are particularly visible on figure 4 for the curves averaged over 100 different CM1 realizations.

As a result, the important conclusions of this section are that 1) the MMSE provides a clear performance advantage compared to a ZF solution, and 2) the simplified MMSE provides a BER similar to the optimal MMSE but avoids inverting a $(2M+1)$-by-$(2M+1)$ matrix.

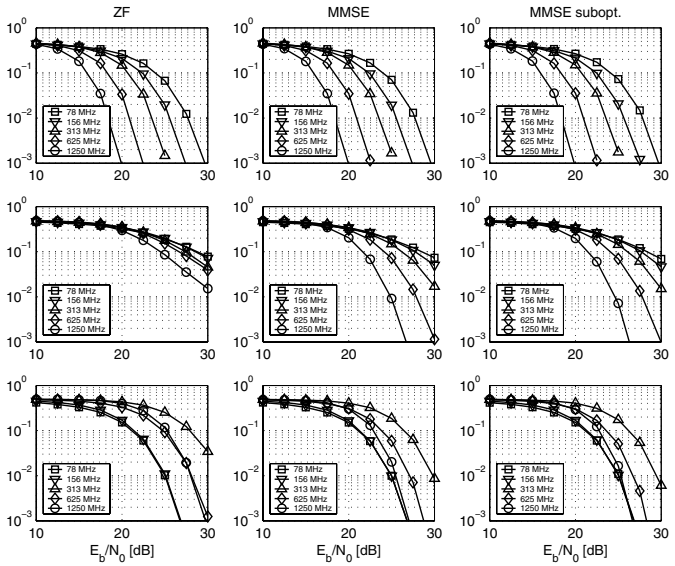

Fig. 4. BER PAM, for AWGN (top), CM1 (middle), CM1 nr. 1 (bottom).

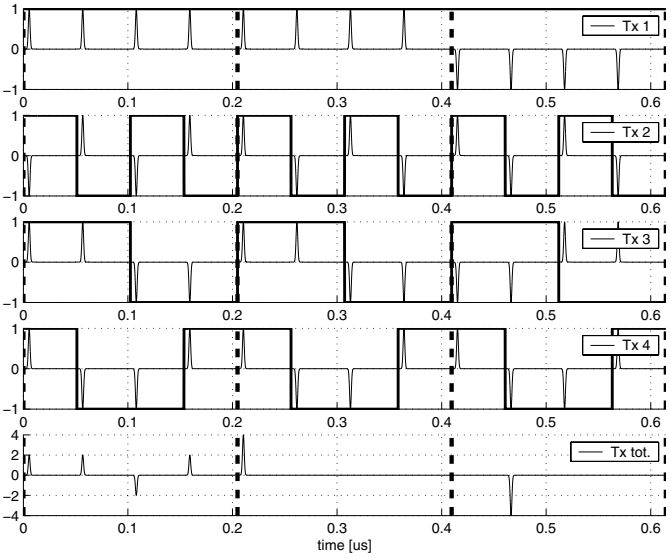

Fig. 5. Channelization technique ($N_c = L_c = 4$), no delay. The Walsh codes and symbol boundaries are shown with bold and dashed lines respectively. In this example, the bits sent on the multiplexed substreams are $\{1, 1, -1\}$, $\{-1, 1, 1\}$, $\{1, 1, -1\}$, $\{1, 1, 1\}$.

III. Orthogonal Multicode Channelization

The BER curves for PAM and PPM indicate that the subsampling receiver is more suitable for lower data rates. Indeed, an important fraction $1-F$ of the signal bandwidth is filtered out, and the pace at which the receiver collects the signal energy is reduced by a factor F. On the other hand, narrowband interference can easily be rejected by avoiding the affected subband (interference excision). Data rates in the order of few Mb/s only can be typically achieved at a pulse repetition rate of 20 MHz. Shorter pulse periods allow reducing the pulse peak amplitude and increasing the data rate, for a given modulation order and signal power. However, this solution is limited by the increased risk of IPI and cannot reach the target date rate of several hundreds of Mb/s.

Instead, we propose to multiplex N_c substreams between two UWB transceivers by means of orthogonal spreading codes of given length $L_c \geq N_c$, such as Walsh codes, applied on top of the classical PN spreading code. The transmitter sends the signal $s_{tx}(t) = \sum_{i=1}^{N_c} s_{tx}^{(i)}(t)$, with

$$s_{tx}^{(i)}(t) = \sum_{n=-\infty}^{+\infty} w^{(i)}\left(t - nL_cT_f\right) \cdot \sum_{k=1}^{K} a^{(i)}_{\lfloor \frac{n}{L_c} \rfloor, k}\, p_{tx}\left(t - nT_f - t^{(i)}_{\lfloor \frac{n}{L_c} \rfloor, k}\right) \quad (8)$$

where $w^{(i)}(t) = \sum_{l=0}^{L_c-1} w_l^{(i)} u(t - lT_f)$ is the Walsh code applied to the ith substream ($w_l^{(i)} \in \{1, -1\}$, $u(t) = 1$ for $0 \leq t \leq T_f$ and 0 otherwise). As in section II, we consider a single user system for the sake of simplicity, and do not take into account the PN spreading in (8).

The receiver recovers the different substreams by applying the different Walsh codes to the received aggregated signal. This approach is similar to the multiplexing of forward-traffic channels in the IS-95 standard, but must be customized here towards the specificity of UWB. Indeed, the transmitted signal resulting from a direct application of this channelization technique leads in worst case to a peak-to-average ratio increased by a factor N_c (fig. 5). This constructive addition may cause harmful interference and complicates the design of the transceivers analog part. It can be avoided by sending the pulses of each substream with a different time offset ϵ_i (fig. 6):

$$s_{tx}^{(i)}(t) = \sum_{n=-\infty}^{+\infty} w^{(i)}\left(t - nL_cT_f\right) \cdot \sum_{k=1}^{K} a^{(i)}_{\lfloor \frac{n}{L_c} \rfloor, k}\, p_{tx}\left(t - nT_f - t^{(i)}_{\lfloor \frac{n}{L_c} \rfloor, k} - \epsilon_i\right) \quad (9)$$

where $\epsilon_i = (i-1)\, T_f / N_c$.

When we consider the impact of the UWB channel on the received signal, however, only partial energy is collected if the receiver despreads the received signal with the Walsh codes used by the transmitter (fig. 7). The tail of the channel energy is lost as the time offset increases, and inter symbol interference (ISI) is introduced. On the other hand, despreading the received signal with appropriately delayed Walsh codes is not appropriate either, since only partial orthogonality is obtained between delayed Walsh codes.

Perfect orthogonality can be achieved using zero-correlation zone (ZCZ) sequences instead of orthogonal codes. The issue of the limited size of code family for long ZCZ is here strongly alleviated by the fact that the zero-correlation zone has a length of 1 chip. A ZCZ multicode approach for UWB was suggested in [16], for example, but ignores the concern of constructive addition between the substreams.

Instead, perfect orthogonality can be obtained with shifted orthogonal codes if the transmitter 1) introduces a cyclic prefix

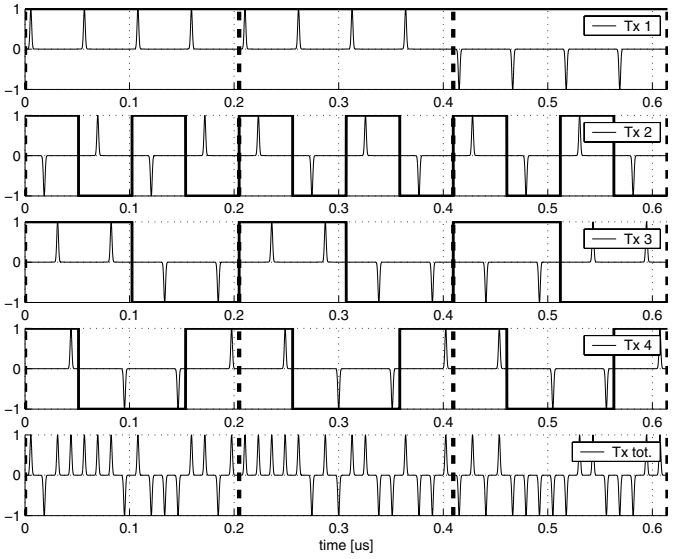

Fig. 6. Channelization technique, delayed substreams.

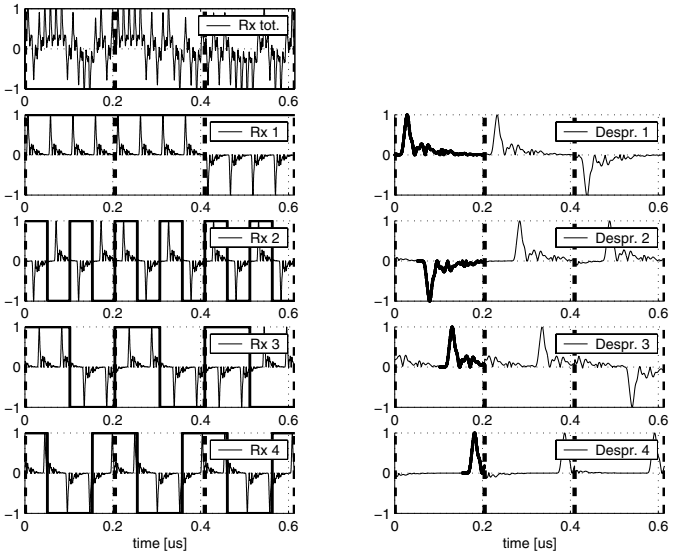

Fig. 7. Contributions of the different substreams to the received signal (left) and suboptimal despread signals (right). The part of the despread signal equal to perfect despreading is shown in bold. For the sake of clarity, we show here a hypothetical despread signal before subsampling.

(CP) in each substream, i.e. inserts at the beginning of each symbol a copy of the last pulse period of the symbol, and 2) applies the same time offset ϵ_i to the $L_c/2-1$ pairs of Walsh codes which only differ by a delay when they are cyclically repeated (such as $w^{(3)}(t)$ and $w^{(4)}(t)$ in the example on fig. 7). The transmitter uses $\lceil N_c/2 \rceil +1$ different delays which are distributed uniformly over $[0, T_f[$ and allocated to the substreams as follows: $[\epsilon_i]_{i=1}^{N_c} = [0, 1, 2, 2, 3, 3, 4, 4, \dots, \lceil N_c/2 \rceil] \cdot T_f/(\lceil N_c/2 \rceil +1)$, assuming $w^{(1)}(t)$ and $w^{(2)}(t)$ are the codes whose cyclic repetition remains orthogonal for any delay (i.e. $w_l^{(1)} = 1$ and $w_l^{(2)} = (-1)^l$, $1 \leq l \leq L_c$). The risk of the small residual constructive addition between the pairs of substreams

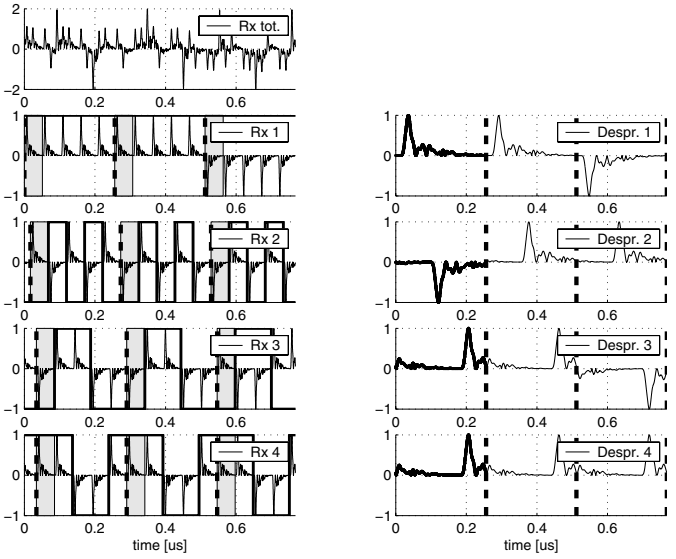

Fig. 8. Contributions of the different substreams to the received signal (left) and optimal despread signals (right). The location of the cyclic prefix in each stream is shown in gray. $[\epsilon_i]_{i=1}^{N_c} = [0, T_f/3, 2T_f/3, 2T_f/3]$.

which share the same value of time offset can easily be reduced, e.g., by using shifted or different PN codes for the two substreams in each of these pairs.

The insertion of the CP prevents ISI at the receiver if the channel impulse response is shorter than the pulse period T_f. It also guarantees the cyclic nature of the L_c pulse periods selected by the receiver after the CP is removed, i.e. orthogonality between the Walsh codes delayed by different time offset values. Compared to a solution based on ZCZ, the cost of the CP is much smaller than the ZCZ sequence length required to achieve the same code family size and multistream capability. Unlike conventional OFDM systems, where the receiver skips periodically a fixed window of received corresponding to the CP, the selection of samples varies here between the substreams.

The delay ϵ_i inserted by the transmitter is easily handled at the receiver by introducing in the frequency domain a phase compensation term $e^{-2\pi j \epsilon_i}$ while equalizing each substream.

We refer to [10] for an overview of the architecture of the subsampling receiver proposed in this paper, and to [17] for a study of the precision requirements of the ADC.

IV. Link Budget

We follow here the guidelines proposed in [18] for UWB link budgets, based on classical narrowband link budgets using Friis transmission formula $P_r = \left(P_t G_t \lambda^2\right) / \left(4\pi d\right)^2$ with geometric average frequency $f_c^{'} = \sqrt{f_{min} f_{max}}$.

The two cases in table I illustrate the link budget for PAM and PPM for different code lengths, assuming a sampling rate equal to $32/T_f$=625 MHz, a target data rate of 110 Mb/s and a channel coding gain of one order of magnitude. The minimum Rx sensitivity level is defined as the minimum required average Rx power for a received symbol in AWGN.

TABLE I

LINK BUDGET FOR LINE SPECTRUM SUBSAMPLING RECEIVER

Term	*case 1*	*case 2*	*Unit*	*Comment*
$R_{b,tot}$	110	110	Mb/s	Bit rate
L_c	16	32	—	Walsh code length
R_b	6.875	3.348	Mb/s	Bit rate for each substream
P_t	-2.5	-2.5	dBm	Tx power per substream
G_t	0	0	dBi	Tx antenna gain
$f_c^{'}$	5.7	5.7	GHz	Geometric central freq.
PL_{1m}	47.6	47.6	dB	Path loss at 1 m and at $f_c^{'}$
PL_{10m}	20	20	dB	Extra loss at $d = 10$m
G_r	0	0	dB	Rx antenna gain
P_r	-70.2	-70.2	dBm	Rx power
N_0	-174	-174	dBm/Hz	Noise PSD
N_b	-105.6	-108.6	dBm	Noise power per bit
NF	7	7	dB	Rx noise figure referred to the antenna terminal [14]
P_n	-98.6	-101.6	dBm/s	Total noise power per bit
(E_b/N_0)	23	23	—	Min E_b/N_0 to reach BER of $1e^{-5}$ (AWGN chan.)
I	2.5	2.5	dB	Implementation loss [14]
M	**3**	**6**	—	Link margin
T_f	50	50	ns	Pulse Period
B	16	16	—	Receiver bandwidth in multiples of T_f^{-1}
f_s	320	320	MHz	Sampling rate
R_{symb}	1.25	0.625	Msymb/s	Symbol rate
b	5.5	5.5	b/symb	Bits per symbol

At a fixed pulse repetition rate, increasing L_c and N_c improves the link budget but does not augment the total data rate. Longer codes increase the number of parallel streams which can be sent *and* the number of pulses per bit. The net data rate is therefore the same but the coding gain has improved. The number of bits per symbol is independent of the Walsh code length, since

$$b = \frac{R_b}{R_{symb}} = \frac{R_{b,tot}/N_c}{1/(L_c T_f)} = \frac{R_{b,tot}/L_c}{1/(L_c T_f)} = R_{b,tot} T_f \qquad (10)$$

Consequently, the two options to increase $R_{b,tot}$ and reach higher data rates are 1) to reduce the pulse period T_f, until the IPI affects the BER performance, 2) to maximize b by resorting to high order PPM and/or PAM, until the link budget becomes negative, requiring longer codes to become again positive. The receiver complexity limits the maximum affordable length and number of codes. N_c parallel streams must indeed be accumulated before being processed by the FFT and the algorithm estimating the pulse position and amplitude.

Channelized streams allow matching dynamically the data rate and quality of service (QoS) according to the user's needs. For a fixed length L_c and a given E_b/N_0, less streams $N_c < L_c$ may be sent if the user's application has temporarily lower requirements in terms of data rate. The power consumption of the transmitter is then reduced by a factor N_c/L_c with respect to the peak transmission power. At the receiver side, less computation power is required to process $N_c < L_c$ streams, which also translates into lower power consumption if appropriate shutdown mechanisms are implemented. When the application requires higher transmission rates, the transmitter sends the data using all possible channels and reaches the peak transmission rate. The information concerning the actual number of codes used by the transmitter can be preliminary sent in a header within the preamble of each packet.

V. CONCLUSIONS

This paper has evaluated different equalization alternatives for a digital based subsampling receiver in the 3.1-10.6 GHz frequency band. Orthogonal channelization techniques are used to achieve high data rates, and accommodate for time-varying rate and QoS requirements of the user, despite low sampling rate. Future work will concentrate on practical implementation aspects and assessment of the power consumption and computational complexity of this receiver.

ACKNOWLEDGEMENT

This work has been developed in the context of the MEDEA+ UPPERMOST project. Y. Vanderperren gratefully acknowledges the financial support from the IWT Belgium.

REFERENCES

[1] R. Hoctor and H. Tomlinson, "Delay-Hopped Transmitted-Reference RF Communications," in *IEEE Conf. on Ultra Wideband Syst. and Technologies*, 2002, pp. 265–270.

[2] B. Le, T. Rondeau, J. Reed, and C. Bostian, "Analog-to-Digital Converters," *IEEE Signal Processing Mag.*, vol. 22(6), pp. 69–77, 2005.

[3] L. Smaini and D. Hélal, "RF Digital Transceiver for Impulse Radio Ultra Wide Band Communications," in *European Solid-State Circuits Conf. (ESSCIRC) Workshop*, 2004.

[4] S. Hoyos, B. Sadler, and G. Arce, "Ultra-Wideband Multicarrier Communication Receiver Based on Analog to Digital Conversion in the Frequency Domain," in *IEEE Wireless Comm. and Netw. Conf.*, 2005.

[5] B. Blazquez, P. Newaskar, F. Lee, and A. Chandrakasan, "A Baseband Processor for Pulsed Ultra-Wideband Signals," in *IEEE Custom Integrated Circuits Conf.*, 2004.

[6] L. Feng and W. Namgoong, "An Oversampled Channelized UWB Receiver," in *IEEE Ultra Wideband Syst. and Technologies*, 2004.

[7] H. Lee, D. Ha, and H. Lee, "Toward digital UWB radios: part I - Frequency Domain UWB Receiver with 1 bit ADCs," in *IEEE Conf. Ultra Wideband Syst. and Technologies,*, 2004, pp. 248–252.

[8] R. Thirugnanam, D. Ha, and S. Choi, "Design of a 4-bit 1.4 GSamples/s Low Power Folding ADC for DS-CDMA UWB Transceivers," in *IEEE Int. Conf. on Ultra-Wideband*, 2005, pp. 536–541.

[9] M. Chen and R. Brodersen, "A Subsampling UWB Impulse Radio Architecture Utilizing Analytic Signaling," *IEICE Trans. Electronics*, vol. E88-C, no. 6, pp. 1114–1121, 2005.

[10] Y. Vanderperren, W. Dehaene, and G. Leus, "A Flexible Low Power Subsampling UWB Receiver Based on Line Spectrum Estimation Methods," in *IEEE Int. Conf. on Comm.*, 2006.

[11] M. Vetterli, P. Marziliano, and T. Blu, "Sampling Signals w. Finite Rate of Innovation," *IEEE Trans. Signal Proc.*, vol. 50, pp. 1417–1428, 2002.

[12] J. Kusuma, A. Ridolfi, and M. Vetterli, "Sampling of Communication Systems with Bandwidth Expansion," in *IEEE Int. Conf. Comm.*, 2002.

[13] J. Zhang, T. Abhayapala, and R. Kennedy, "Principal Components Tracking Algorithms for Synchronization and Channel Identification in UWB Systems," in *IEEE Eighth Int. Symposium on Spread Spectrum Techniques and Applications*, 2004, pp. 369–373.

[14] J. Foerster, "Channel Modeling Sub-Committee Report Final (IEEE P802.15-02/490r1-SG3a)," 2003.

[15] I. Maravić and M. Vetterli, "Low-Complexity Subspace Methods for Channel Estimation and Synchronization in Ultra-Wideband Systems," in *Int. Workshop on UWB Systems*, 2003.

[16] D. Wu, P. Spasojević, and I. Seskar, "Ternary Zero-Correlation Zone Sequences for Multiple Code UWB," in *38th Conf. on Information Sciences and Syst.*, 2004, pp. 939–943.

[17] Y. Vanderperren, G. Leus, and W. Dehaene, "An Approach for Sprecifying the ADC and AGC Requirements for UWB Digital Receivers," in *IET Seminar on UWB Systems, Technologies and Applications*, 2006.

[18] K. Siwiak, J. Ellis, and R. Roberts, "802.15.3TGa Alternate PHY Selection Criteria (IEEE P802.15-03/031r5)," 2002.